Electronic Supplementary Information

Designed synthesis of SiC nanowire-derived carbon with dual-scale nanostructures for supercapacitor applications

Xingli Zou,*[ab†] Li Ji,[bc†] Hsien-Yi Hsu,[de†] Kai Zheng,[a] Zhongya Pang[a] and Xionggang Lu*[a]

a. State Key Laboratory of Advanced Special Steel & Shanghai Key Laboratory of Advanced Ferrometallurgy & School of Materials Science and Engineering, Shanghai University, Shanghai 200072, China.

b. Center for Electrochemistry, Department of Chemistry, The University of Texas at Austin, Austin, Texas 78712, United States.

c. Microelectronics Research Center, Department of Electrical and Computer Engineering, The University of Texas at Austin, Austin, Texas 78712, United States.

d. School of Energy and Environment, City University of Hong Kong, Hong Kong, China.

e. Shenzhen Research Institute of City University of Hong Kong, Shenzhen 518057, China.

† *These authors contributed equally.*

* *Corresponding Author: xinglizou@shu.edu.cn (X. Zou); luxg@shu.edu.cn (X. Lu)*

Outline

Experimental details

1. Chemicals

SiC nanowires (NWs) and TiC micro/nanoparticles were electrosynthesized from nanoscale SiO_2 (approximately 50-100 nm), TiO_2 (approximately 500 nm), and C (approximately 500 nm) powders. Polyvinyl butyral, anhydrous calcium chloride ($CaCl_2$), calcium oxide (CaO), and anhydrous ethanol were used in experiments. In addition, CO_2 gas was also used as carbon resource for the synthesis of SiC ($SiO_2/CO_2 \rightarrow SiC$) in this work. These chemicals were analytical reagents and purchased from Sinopharm Chemical Reagent Co., Ltd, China. All chemicals were used as received without further purification. Deionized water was used in experiments.

2. Fabrication of SiO_2/C cathode

The starting metal oxides and carbon powders with approximately 1–2 wt % polyvinyl butyral binder were mixed at the predesigned molar ratios (SiO_2:C = 1:1 and TiO_2:C = 1:1) corresponding to the target/pre-designed products (SiC and TiC) and homogenized by ball milling. Then, the milled mixtures were pressed under 10–15 MPa to form porous SiO_2/C and TiO_2/C pellets. These pressed pellets precursors, with appropriate open porosities (SiO_2/C (~28.1%); TiO_2/C (~29.2%)) were attached to electrode wire and then served as cathode precursors for the electrosynthesis of their corresponding metal carbides (MCs) *i.e.*, SiC and TiC, respectively. The cathode pellets were pre-sintered during the heating process with furnace, which have been proved in our experiments that the pellets can obtain sufficient mechanical strength for the subsequent electroreduction process. It should be noted that, in this experiment, ~2.0 g SiO_2/C porous pellet was used as the cathode precursors for the electrosynthesis of SiC NWs.

3. Fabrication of the solid oxide membrane (SOM)-based anode and its key feature

The key feature of the SOM-assisted controllable electroreduction process is the use of an SOM-based anode system. The SOM-based anode system consists of a one-end-closed 8 mol % yttria-stabilized zirconia (YSZ) tube filled with carbon-saturated liquid metal (tin or copper), and a Mo/Fe-Cr-Al wire was inserted into the assembled YSZ tube to conduct electricity. The SOM-assisted controllable electroreduction process typically possesses considerable current efficiency.[1-4] This process has been successfully employed to produce metals, alloys, and composites with considerable advantages.[1-4] Actually, if hydrogen is passed through the SOM-based anodic reaction area where it oxidizes the oxygen ions to form water vapor, or direct oxidizes the oxygen ions at the SOM-based

anodic reaction area by novel metal such as liquid silver to form oxygen gas,[3] this process has the potential to realize green and sustainable production.[1-4]

4. Molten salt (MS) electroreduction/electrochemical experiments

MS electroreduction experiments were systematically carried out using the assembled SOM-based anode system, as shown in Fig. S1, which can also be found in our previous work.[1,2,4] The fabricated cathode (MOs/C) precursors and the SOM-based anode system were assembled in an alumina crucible to form an electrolytic cell. When the system temperature reached the experimental temperature (1000 °C), appropriate constant potential would be applied between the cathode and the SOM-based anode system in the assembled electrolytic cell. The applied potential should exceed the dissociation potential of metal oxides at the experimental temperature. In the SOM-based anode system experiment, 4.0 V was chosen as the applied potential in order to obtain sufficient reaction driving force and reaction speed. Importantly, the applied potential 4.0 V has been proved to be suitable for the formation of homogeneous SiC NWs structures in this experiment. It should be noted that the applied potential of the SOM-assisted controllable electroreduction process can be increased as long as the potential drop across the SOM tube and the molten salt does not exceed the dissociation potential of the zirconia (approximately 2.0 V) as well as the molten $CaCl_2$ (approximately 3.2 V), respectively. The inevitable potential drop across the SOM tube can be affected by various parameters, such as the thickness of the SOM and temperature, *etc*. Therefore, the applied potential 4.0 V in this SOM-assisted controllable electroreduction process can only be considered as general guidelines for the formation of SiC NWs, different electrolytic systems require different applied potentials to generate homogeneous SiC NWs structures. During electroreduction process, oxygen component was gradually electroreduced and migrated through MS and membrane then to the SOM-based anode system, where it was oxidized by carbon to form CO/CO_2 gases. Simultaneously, MCs including SiC NWs and TiC were electrosynthesized at the cathode. It should be noted that the SOM-assisted controllable electroreduction process consumes only electrons during the entire synthesis process. Considering electrons can be generated from green/renewable energy sources such as solar energy and wind energy (Fig. S1), the SOM-assisted controllable electroreduction process has the potential to provide a sustainable route for the synthesis of MCs and MAX phases materials. After the SOM-assisted controllable electroreduction process, the electrolytic system can immediately entry the subsequent *in-situ* molten salt electrochemical etching process to produce carbide-derived carbons (CDCs) by only

changing the electrodes and the applied potential (see section 5. Electrochemical etching experiments).

Moreover, electrochemical conversion of CO_2 and SiO_2 to SiC in $CaCl_2$-based molten salt has also been preliminarily carried out in this work. During the SOM-assisted electroreduction process, $CaCl_2$-CaO molten salt was used as electrolyte, CO_2 was continuously purged into the molten electrolyte, and the pressed porous SiO_2 pellet was used as cathode precursor. CO_2 can be captured by the $CaCl_2$-CaO molten salt and electrolyzed to carbon as reported in the previous work.[5] Therefore, electroreduction of SiO_2 and CO_2 could be simultaneously happened during the electrolysis process, CO_2 could be served as carbon resource for the synthesis of SiC, and the general reaction is $SiO_2 + CO_2 + 8e^- \rightarrow SiC + 4O^{2-}$. Consequently, CO_2 and SiO_2 could be electrochemically converted into SiC through electroreduction and carbonization processes. The other experimental procedures were also same with the experimental procedures involved in the SOM-based anode electroreduction process as described above.

Cyclic voltammetry (CV) experiments were carried out in three-electrode electrolytic system, in which a metallic cavity electrode (MCE)[6,7] filled with metal oxides/carbon (MOs/C) powder was used as working electrode, a Pt wire and the SOM-based anode were served as reference electrode and counter electrode, respectively. Before the CV experiments, the electrolytic cell was pre-electrolyzed at 2.5 V for 3–5 h to remove the residual moisture and other redox-active impurities. A Biologic HCP-803 electrochemical workstation was used for the CV experiments.

5. Electrochemical etching experiments

To further evaluate the proposed route for the electrochemical production of CDCs in MS, a subsequent *in-situ* electrochemical etching process was carried out in the molten salt after the MCs electrosynthesis experiments. After the MCs have been completely electrosynthesized from their MOs/C precursors, the obtained MCs products such as the nanostructured SiC and TiC were then served as carbides precursors to produce CDCs using the *in-situ* electrochemical etching process. For the *in-situ* electrochemical etching experiments, the electrodes were changed: the electrosynthesized MCs were functioned as the anode, a graphite rod (or other metallic electrode such as Ni) was inserted into the molten electrolyte and served as the cathode, and potential of 2.5–3.0 V was applied between the MCs electrode and the graphite electrode (or other metallic electrode such as Ni). The electrochemical etching time can be controlled to synthesize partially etched MCs@CDCs structures or completely etched pure porous CDCs. A Biologic HCP-803 electrochemical workstation was also used to control the electrochemical etching experiments. After the etching experiment, the furnace was

cooled down to room temperature, and then the etched products were washed with distilled/deionized water and dried.

The reaction mechanism of the electrochemical etching of MCs can be generally expressed as following:

$MC - ne^- \rightarrow M^{n+} + C$ (CDCs), at the anode;

$M^{n+} + ne^- \rightarrow M$, at the cathode, indicating the metallic elements (M) contained in the MCs can be reproduced as electrodeposits. We note that calcium oxide plays an important role during the etching process (*e.g.*, the formation of SiO_y^{n-}, and then the silicate ions were electrodeposited at cathode).

CV experiments for the electrochemical etching process were also carried out in three-electrode electrolytic system, in which the electrosynthesized SiC NWs was used as working electrode, a Pt wire and a graphite-based anode were served as reference electrode and counter electrode, respectively. Before the CV experiments, the molten $CaCl_2$ was pre-electrolyzed at 2.5 V for 3–5 h to remove the residual moisture and other redox-active impurities. A Biologic HCP-803 electrochemical workstation was used for the CV experiments.

Figures S1-S22, Table S1 and Reactions (S1)-(S16)

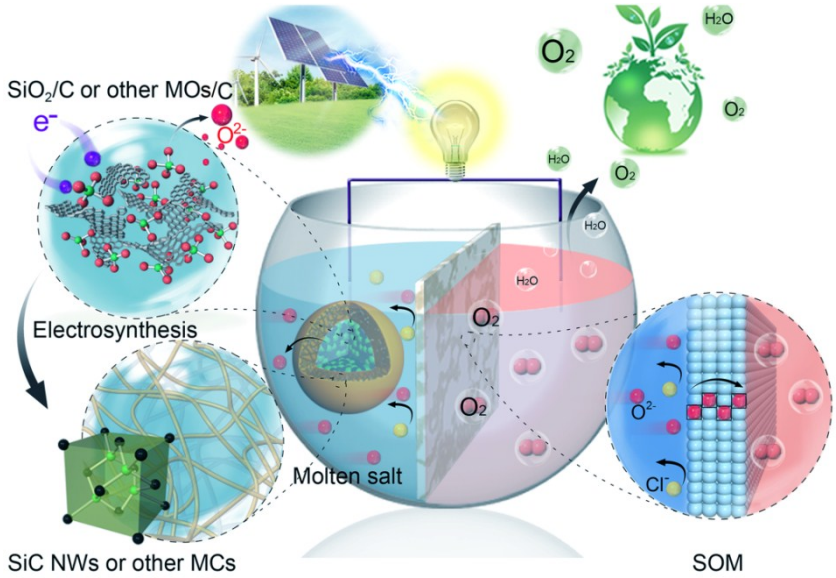

Figure S1 Schematic illustration of the SOM-assisted molten salt electrolytic cell used for the synthesis of SiC NWs and MCs nanoparticles (NPs) from MOs/C precursors.

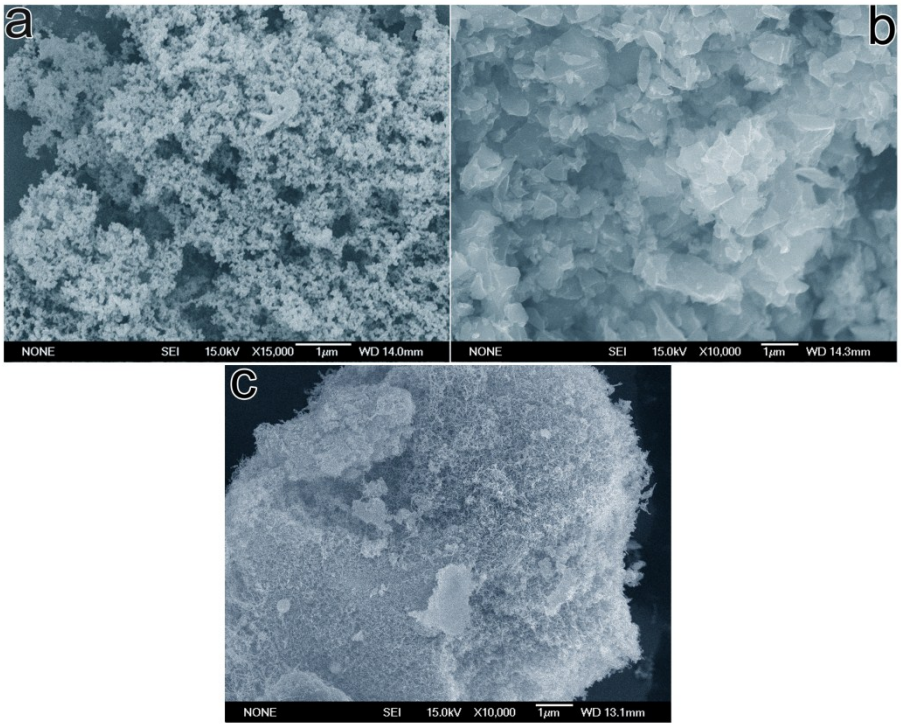

Figure S2 (a) and (b) SEM images of (a) SiO_2 and (b) carbon powders precursors used for the electrosynthesis of SiC NWs. (c) SEM image of the bulk SiC NWs synthesized using the SOM-assisted controllable electroreduction process (1000 °C, 4.0 V, 6 h, 2.0 g SiO_2/C as precursors).

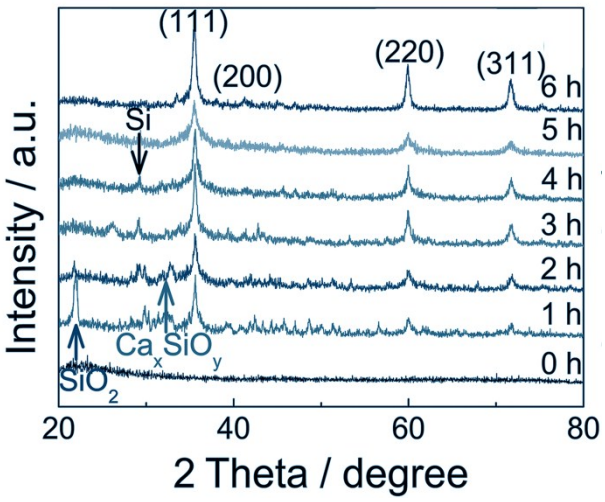

Figure S3 XRD analysis showing the phase composition variations during the synthesis process for SiC NWs in molten $CaCl_2$ at 1000 °C and 4.0 V.

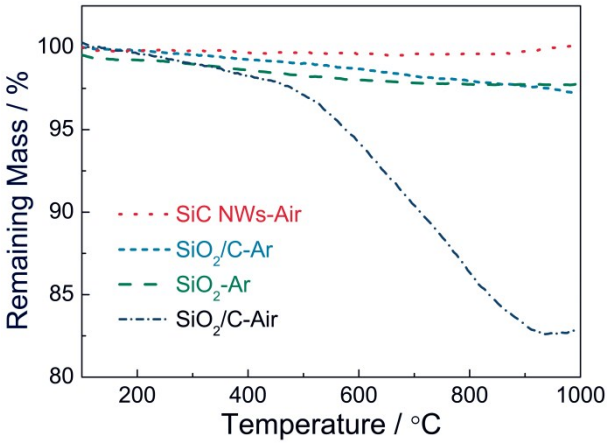

Figure S4 TG curves of the SiO_2/C precursors and the electrosynthesized SiC NWs (obtained by using the SOM-assisted controllable electroreduction process, 1000 °C, 4.0 V, 6 h) with a heating rate of 10 °C min^{-1} up to 1000 °C in air or Ar gas.

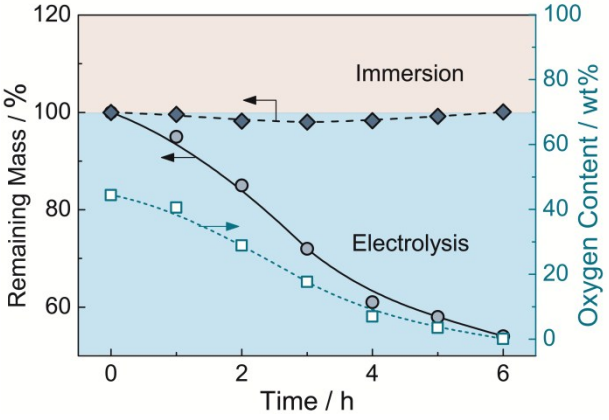

Figure S5 Weight changes of SiO_2/C precursors during the SOM-assisted controllable electroreduction process (1000 °C, 4.0 V) and immersion process (1000 °C, without applied potential) in molten $CaCl_2$, and the variation of oxygen content of SiO_2/C cathode with electroreduction time during the SOM-assisted controllable electroreduction process (1000 °C, 4.0 V).

During the electroreduction process, the trends of weight change and oxygen content variation are similar. In the time period of 0 to ~1 h, the electroreduction-generated O^{2-} can partially react with SiO_2 and Ca^{2+} to form $CaSiO_3$ in molten $CaCl_2$, *i.e.*, $SiO_2 + Ca^{2+} + O^{2-} \rightarrow CaSiO_3$,[7] therefore, the oxygen content decreases slowly. However, the formed $CaSiO_3$ can dissolve in molten $CaCl_2$ immediately to form SiO_3^{2-},[7,8] and then SiO_3^{2-} and C can be further converted into SiC NWs through electrodeposition and carbonization processes (details will be discussed in Fig. S9).

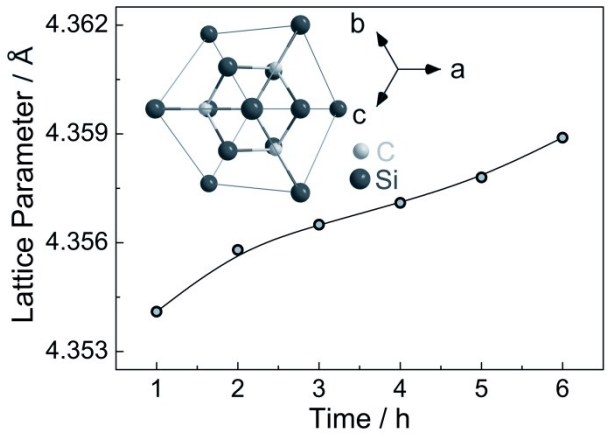

Figure S6 Changes of the lattice parameter (calculated based on the XRD analysis) of the synthesized SiC phase with electroreduction time during the SOM-assisted controllable electroreduction process (1000 °C, 4.0 V), the inset is schematic representation of the 3C-SiC crystal structure along the [111] zone axis.

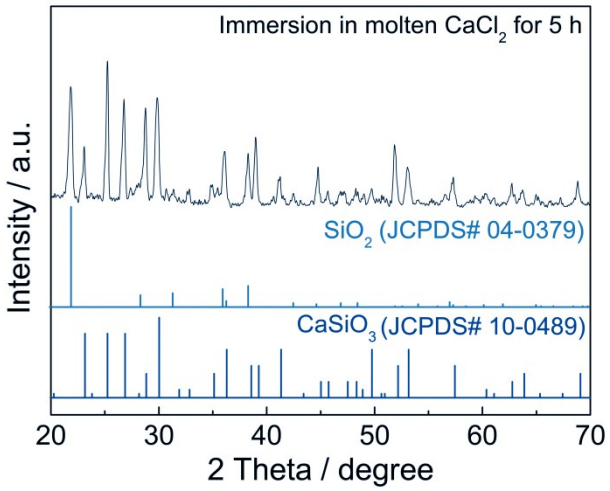

Figure S7 XRD pattern of the surface of the SiO_2/C pellet precursors after being immersed in molten $CaCl_2$ at 1000 °C for 5 h without applied potential.

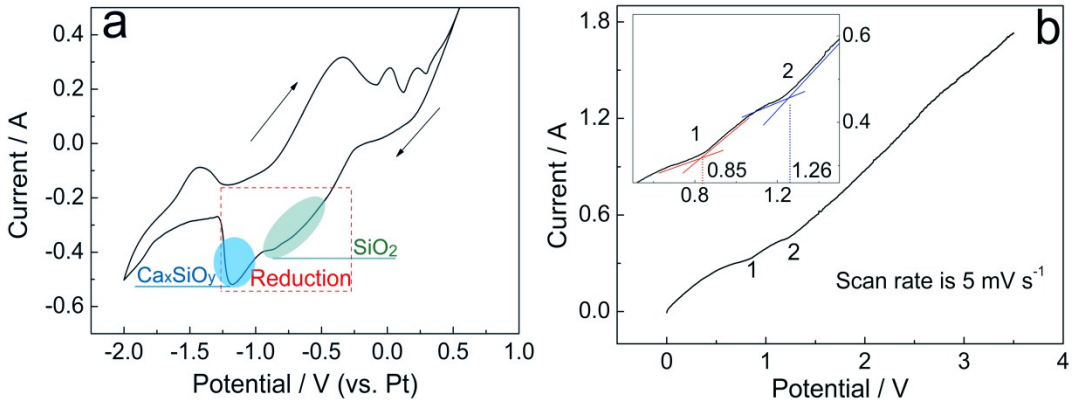

Figure S8 (a) CV curve of SiO_2/C precursors in molten $CaCl_2$ at 1000 °C using the SOM-based anode system with a scan rate of 60 mV s^{-1}. (b) The slow potentiodynamic scan of SiO_2/C precursors in molten $CaCl_2$ at 1000 °C using the SOM-based anode system with a scan rate of 5 mV s^{-1}.

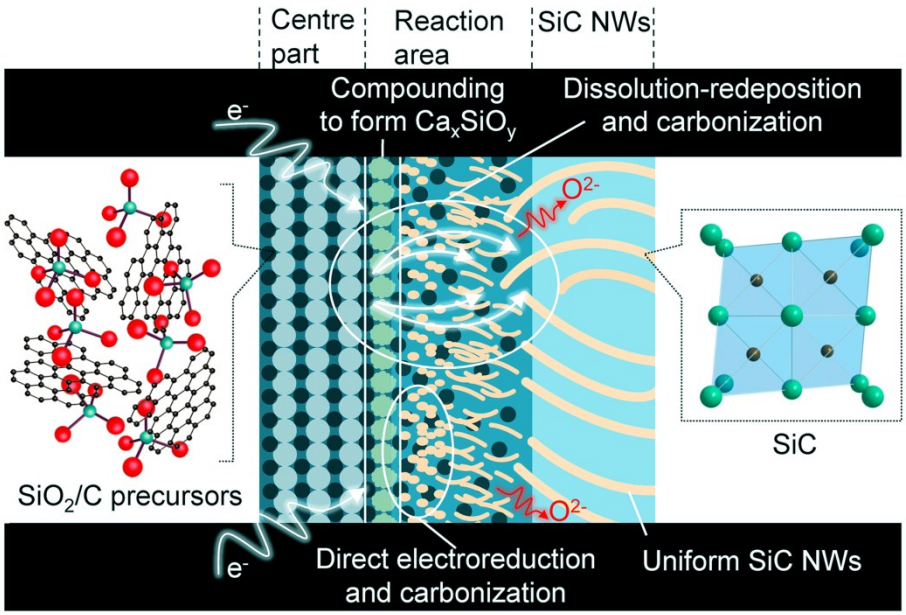

Figure S9 Schematic illustration showing the reaction mechanism of the electrosynthesis of SiC NWs from SiO_2/C precursors in molten $CaCl_2$.

Firstly, Ca_xSiO_y can be generated through the chemical/electrochemical compounding reactions (reactions (S1)-(S3)) during the immersion and electroreduction processes in molten $CaCl_2$.[7,8] It should be noted that the CaO component may be ascribed to the reaction ($CaCl_2$•(H_2O) → CaO + 2HCl) due to $CaCl_2$ can easily absorb moisture during the experimental assembly process.[7] Simultaneously, SiO_2/C powders and the formed calcium-enriched compounds Ca_xSiO_y/C mixture can be directly electroreduced to initial SiC NPs/nuclei through electroreduction and *in-situ* carbonization reactions (reactions (S2)-(S7)). In addition, Ca_xSiO_y can dissolve in molten $CaCl_2$ to form SiO_y^{n-}, which can electrodeposit on the electroreduction-generated SiC particles/nuclei and then further reacts with C to form initial SiC NWs structures in the reaction area (reactions (S8) and (S9)). With the reaction area gradually extends into the center part of SiO_2/C pellet precursors, the compounding, direct

electroreduction, dissolution-electrodeposition, and *in-situ* carbonization processes coexist in the reaction area and promote the initial SiC NWs/NPs grow up to form homogeneous SiC NWs. Therefore, the reaction pathway from SiO_2/C to SiC NWs can be generally summarized as: SiO_2/C → Ca_xSiO_y, C, Si, SiC → SiC NWs. It should be noted that the electroreduction process can leave voids in the products to form porous structure,[9,10] which is important for the dissolution-electrodeposition mechanism[7,9,10] and the formation of porous NWs structures. In addition, appropriate applied potential (overpotential) is also very important for the electrosynthesis of SiC NWs. The overpotential can influence the reaction speed and the crystal nucleation and growth during the electroreduction and the dissolution-electrodeposition processes.[7]

Therefore, the reaction route typically involves chemical/electrochemical compounding processes (reactions (S1)-(S3)), electroreduction/carbonization processes (reactions (S2)-(S7)), and dissolution/electrodeposition/carbonization processes (reactions (S8) and (S9)), *i.e.*,

Chemical/electrochemical compounding processes and electroreduction/carbonization processes:

$$SiO_2 + CaO \,/\, 2CaO\ (Ca^{2+}, O^{2-}) \rightarrow CaSiO_3 \,/\, Ca_2SiO_4 \quad \text{(S1)}$$

($\Delta G^0_{CaSiO3\ (1000\ °C)} = -136.34$ kJ mol^{-1}, $\Delta G^0_{Ca2SiO4\ (1000\ °C)} = -135.48$ kJ mol^{-1})

$$2SiO_2 + Ca^{2+} + 4e^- + C \rightarrow CaSiO_3 + O^{2-} + SiC \quad \text{(S2)}$$

$$2SiO_2 + 2Ca^{2+} + 4e^- + C \rightarrow Ca_2SiO_4 + SiC \quad \text{(S3)}$$

Electroreduction/carbonization processes:

$$SiO_2 + 4e^- + C \rightarrow 2O^{2-} + SiC \quad \text{(S4)}$$

$$CaSiO_3 + 4e^- + C \rightarrow Ca^{2+} + 3O^{2-} + SiC \quad \text{(S5)}$$

$$Ca_2SiO_4 + 4e^- + C \rightarrow 2Ca^{2+} + 4O^{2-} + SiC \quad \text{(S6)}$$

$$Si + C \rightarrow SiC\ (\Delta G^0_{1000\ °C} = -63.16\ \text{kJ mol}^{-1}) \quad \text{(S7)}$$

Dissolution/electrodeposition/carbonization processes:

$$CaSiO_3 \,/\, Ca_2SiO_4 \rightarrow SiO_y^{n-} + Ca^{2+} \quad \text{(S8)}$$

$$SiO_y^{n-} + C + 4e^- \rightarrow yO^{2-} + SiC \quad \text{(S9)}$$

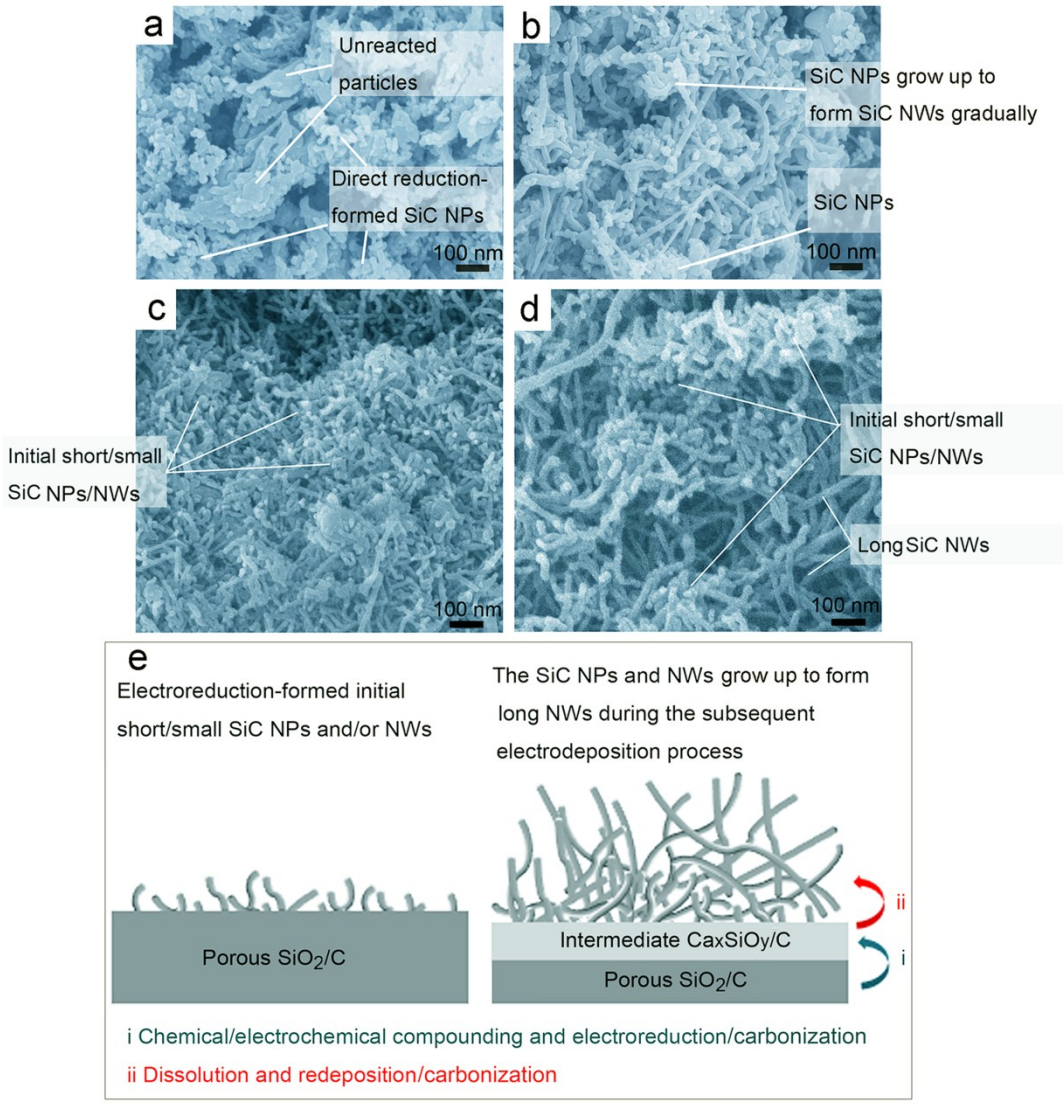

Figure S10 SEM images and schematic illustration showing the "SiC NPs → SiC NWs" growth process. (a)-(d) SEM images of the SiC products electrosynthesized using the SOM-assisted controllable electroreduction process at 1000 °C and 4.0 V for (a) 2 h, (b) 3 h, (c) 4 h, (d) 5 h. (e) Schematic illustration showing the SiC NWs formation/growth processes.

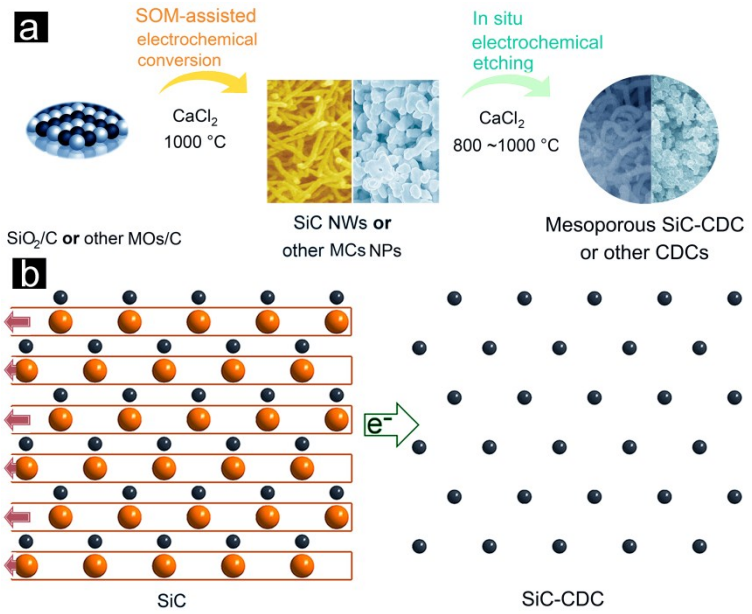

Figure S11 (a) Schematic illustration of the new proposed route for the electrosynthesis of micro/nanostructured MCs (such as SiC NWs) and their porous CDCs (such as SiC-CDCs) in $CaCl_2$-based molten salt (MOs/C → MCs → CDCs). (b) Schematic showing the electrochemical etching of SiC to produce SiC-CDCs.

The proposed route consists of two periods, *i.e.*, (i) the SOM-assisted controllable electroreduction of MOs/C to produce micro/nanostructured MCs; (ii) *in-situ* electrochemical conversion of the as-synthesized MCs to produce porous CDCs *via* electrochemical etching. The SOM-assisted controllable electroreduction process can produce high-purity MCs without any residual carbon, which is important for the synthesis of high-quality CDCs through the subsequent *in-situ* electrochemical etching process. The route allows us to produce a wide variety of micro/nanostructured MCs, CDCs/MCs composites, and pure porous CDCs by strictly controlling the electrosynthesis condition. Considering the electroreduction process can be carried out in various molten salts such as $CaCl_2$-NaCl, $CaCl_2$, *etc.*,[6,7] it is thus reasonable to believe that the proposed route can also be carried out in various molten salts, and the experimental temperature can also be further decreased to low temperature.

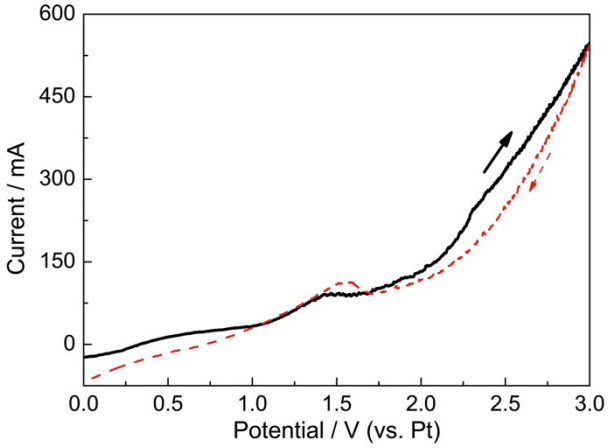

Figure S12 CV curve of the synthesized SiC NWs during the electrochemical etching process in molten $CaCl_2$ at 1000 °C with a scan rate of 5 mV s^{-1}.

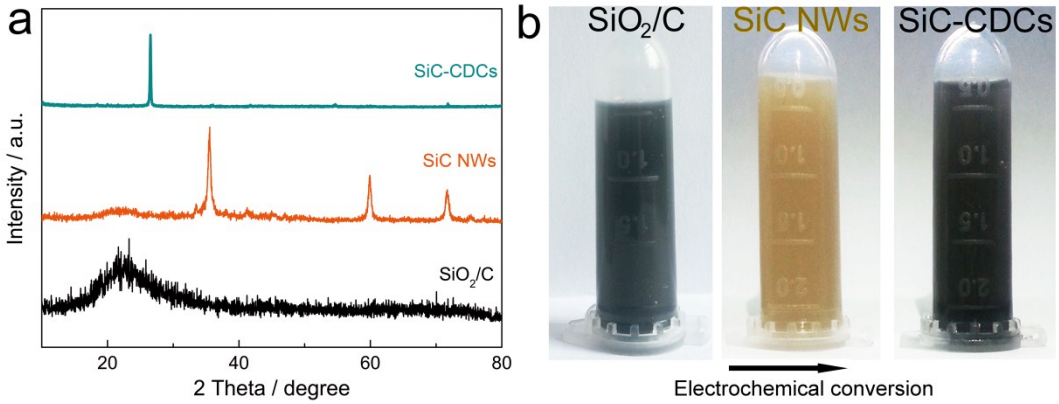

Figure S13 (a) XRD patterns of the SiO_2/C precursors, the as-synthesized SiC NWs (1000 °C, 4.0 V, 6 h), and the electrochemical etching-produced SiC-CDC NWs (1000 °C, 3.0 V, 12 h). (b) Photos of the SiO_2/C precursors, the synthesized SiC NWs, and the obtained SiC-CDC NWs dispersed in water.

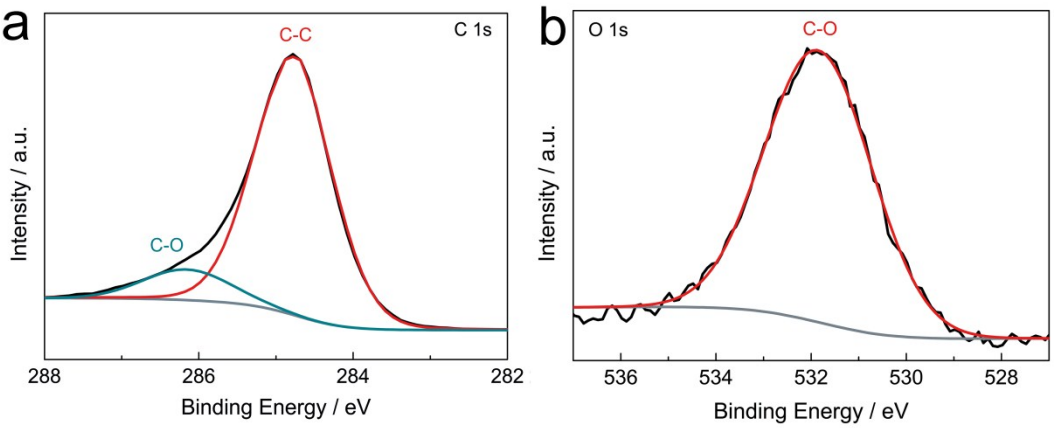

Figure S14 (a and b) Representative XPS spectra of (a) C 1s and (b) O 1s regions, which correspond to Figure 4c.

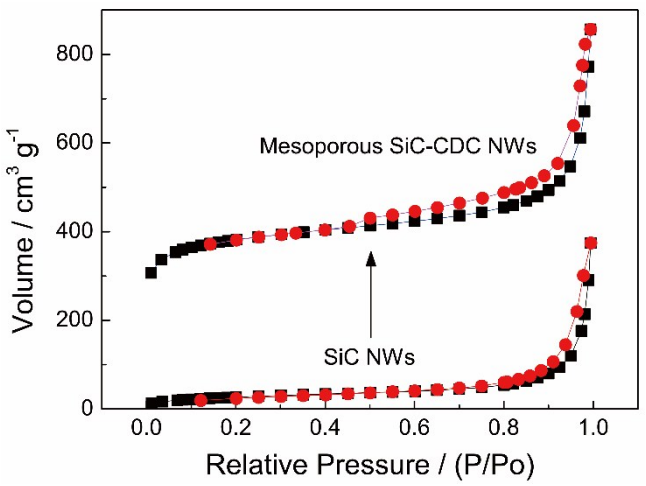

Figure S15 Nitrogen adsorption-desorption isotherms of the as-synthesized SiC NWs and SiC-CDC NWs.

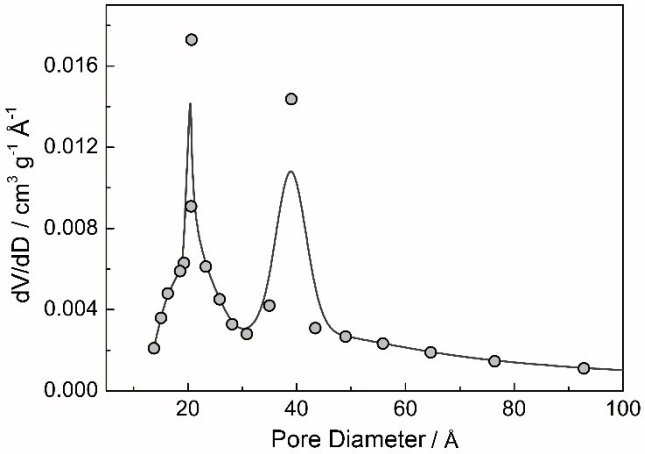

Figure S16 Pore size distribution of the as-synthesized SiC-CDC NWs, which correspond to Fig. 4d.

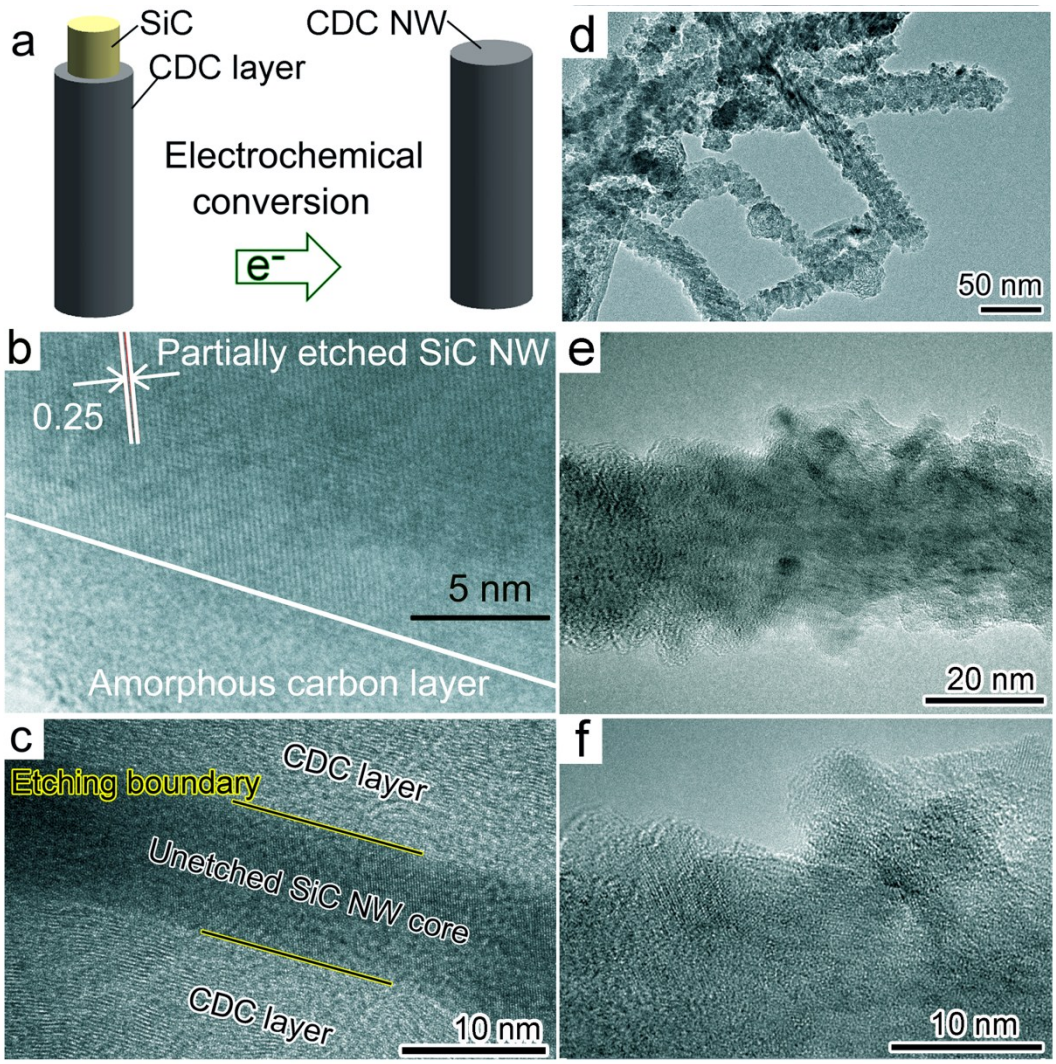

Figure S17 (a) Schematic illustration showing the electrochemical etching process for synthesis SiC-CDC NWs. (b and c) Typical TEM images of the partially etched SiC NWs, which exhibit the SiC NW@CDC structures. (d-f) TEM and HRTEM images showing the typical unique SiC-CDC NW structure observed in the as-obtained SiC-CDC NWs product.

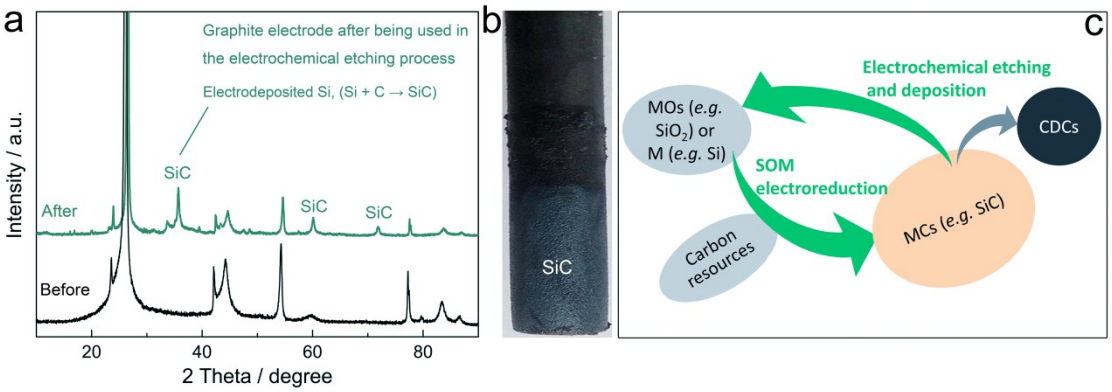

Figure S18 (a) XRD patterns of the surfaces of the graphite-based electrode before and after being used in the electrochemical etching experiment. (b) Photo of the graphite electrode after being used in the electrochemical etching experiment. (c) Schematic illustration showing the cyclic diagram of the proposed route for CDCs materials synthesis.

Obviously, SiC has been observed on the surface of the graphite electrode after being used in the electrochemical etching experiment, indicating that the reaction mechanism of the electrochemical etching process generally contains the reactions, *i.e.*, $SiC - 4e^- \rightarrow Si^{4+} + C$ (CDCs, anodic reaction) and $Si^{4+} + 4e^- \rightarrow Si$ (cathodic reaction). It is suggested that Si^{4+} has been extracted from SiC during the electrochemical etching process, and then the Si^{4+} electrodeposited on the surface of the graphite electrode, the deposited Si further reacted with the graphite electrode to form SiC again on the electrode surface. These results indicate that the metal (M) elements (such as Si) contained in the MCs (such as SiC) can be redeposited/recovered at the electrode as electrodeposits during the electrochemical etching process, which means that the M elements can be severed as the intermediates, and the proposed route has the potential to realize cyclic production of CDCs materials.

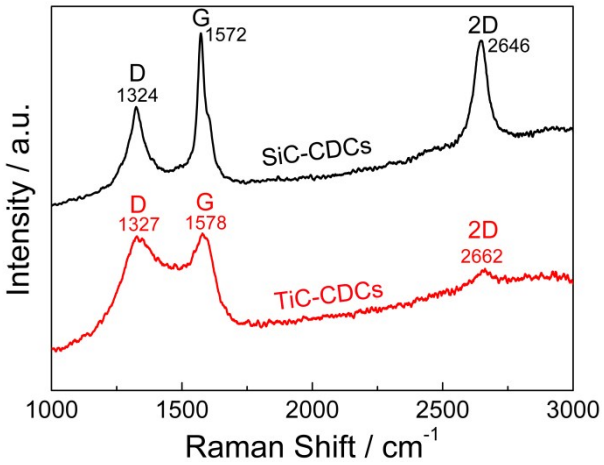

Figure S19 Comparison of the typical Raman spectra of the SiC-CDC (1000 °C, 3.0 V, 12 h) and TiC-CDC (1000 °C, 3.0 V, 12 h) electrosynthesized using the proposed route.

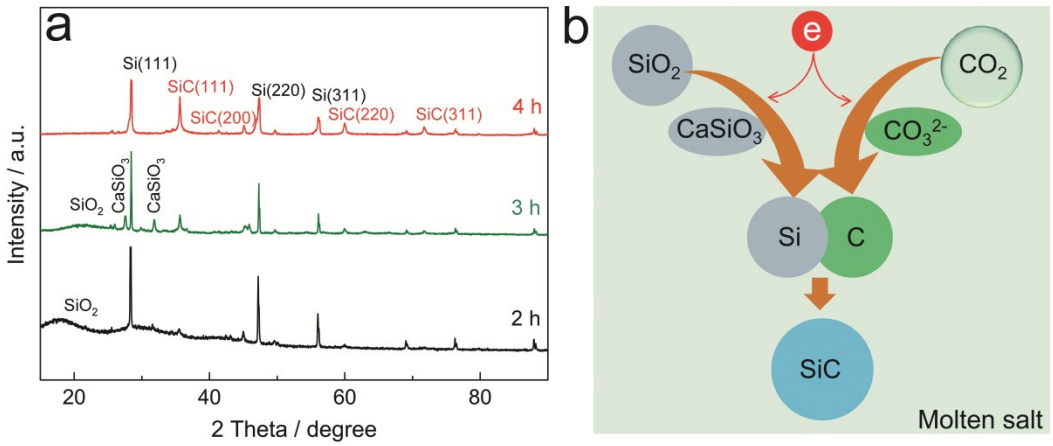

Figure S20 (a) XRD patterns of the products obtained from SiO_2 and CO_2 (captured by molten salt and served as carbon source) at different times. (b) Schematic illustration of the sustainable route from SiO_2/CO_2 to SiC.

The previous work[7,11,12] suggested that CO_2 can be converted into C by electrolysis in molten salts *via* reactions (S10) and (S11).

$$O^{2-} + CO_2\,(g) \rightarrow CO_3^{2-} \quad \text{(S10)}$$

$$CO_3^{2-} + 4e^- \rightarrow C + 3O^{2-} \quad \text{(S11)}$$

Therefore, it is suggested that the C product converted from CO_2 has the potential to be used for the *in-situ* synthesis of MCs. The reaction mechanism of the electrochemical conversion of MO_s/CO_2 to MCs in $CaCl_2$-based molten salts can be generally expressed by reactions (S12)-(S16).

$$nM_\alpha O_\beta + 2(n\beta+2n\alpha)e^- + n\alpha CO_2 \rightarrow n\alpha MC + (n\beta+2n\alpha)O^{2-} \quad \text{(S12)}$$

$$nM_\alpha O_\beta + \varphi CaO \rightarrow Ca_\varphi M_{n\alpha} O_{(n\beta+\varphi)} \quad (\varphi > 0) \quad \text{(S13)}$$

$$Ca_\varphi M_{n\alpha} O_{(n\beta+\varphi)} + 2(n\beta+2n\alpha)e^- + n\alpha CO_2 \rightarrow n\alpha MC + \varphi CaO(Ca^{2+},\ O^{2-}) + (n\beta+2n\alpha)O^{2-}\ (\varphi > 0)\ (\text{S14})$$

$$nM_\alpha O_\beta + [\beta(n\alpha-\delta)/\alpha - \psi]Ca^{2+} + [2\beta(n\alpha-\delta)/\alpha + 4(n\alpha-\delta)]e^- + (n\alpha-\delta)CO_2 \rightarrow Ca_{[\beta(n\alpha-\delta)/\alpha - \psi]} M_\delta O_{(n\beta-\psi)} + (n\alpha-\delta)MC + [\psi + 2(n\alpha-\delta)]O^{2-} \quad (n\alpha > \delta > 0,\ \psi \geq 0) \quad \text{(S15)}$$

$$Ca_{[\beta(n\alpha-\delta)/\alpha - \psi]} M_\delta O_{(n\beta-\psi)} + (2\beta\delta/\alpha + 4\delta)e^- + \delta CO_2 \rightarrow \delta MC + (n\beta-\psi+2\delta)O^{2-} + [\beta(n\alpha-\delta)/\alpha - \psi]Ca^{2+} \quad (n\alpha > \delta > 0,\ \psi \geq 0) \quad \text{(S16)}$$

On the basis of the XRD analysis (Fig. S20) and the above discussion, it can be concluded that the electrochemical conversion of SiO_2/CO_2 to SiC is possible, and the conversion process includes the electroreduction process and carbonization process. We are continuing our studies to investigate more details of the electrochemical conversion process from CO_2 to CDCs, and further investigations will be reported in due course.

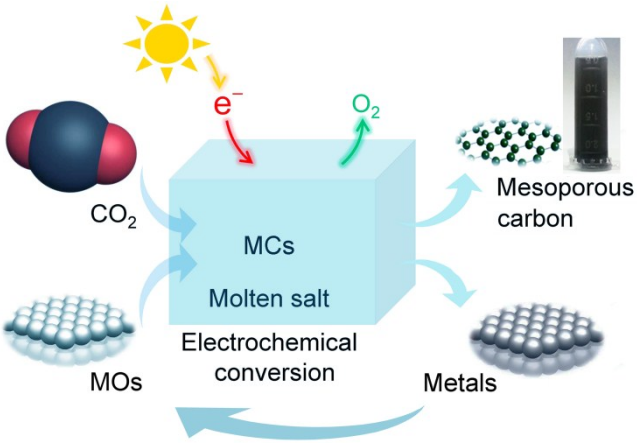

Figure S21 Schematic illustration of the proposed possible sustainable route for the electrochemical conversion of CO_2 to micro/nanostructured mesoporous carbon materials. The proposed route has the potential to realize sustainable and cyclic production of CDCs materials.

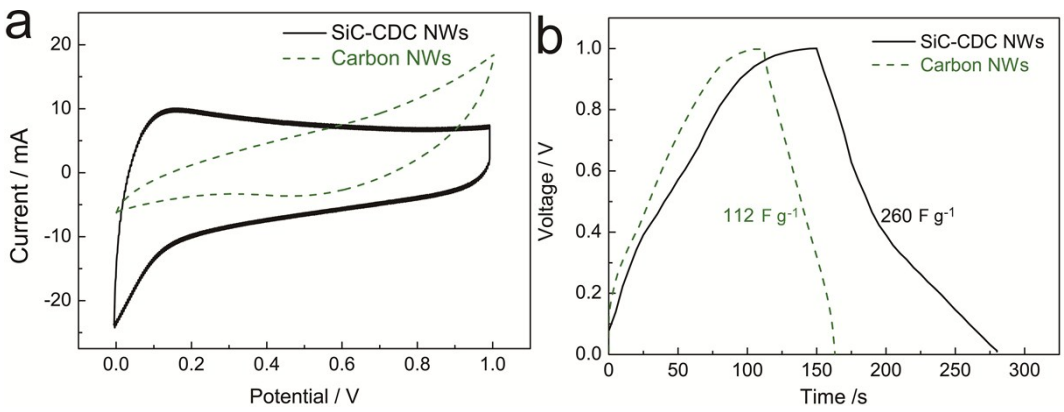

Figure S22 (a) CV curves of the SiC-CDC NWs with mesopores and carbon NWs without mesopores in 6 M KOH electrolyte with scan rate of 20 mV s^{-1}. (b) Charge-discharge curves of the SiC-CDC NWs and carbon NWs measured at current density of 1 A g^{-1}.

Table S1 Specific capacitance of the synthesized SiC-CDC NWs compared with other typical carbon materials in 6 M KOH aqueous solution.

Carbon-based electrodes	S_{-BET} (m^2 g^{-1})	Specific capacitance (F g^{-1})	Reference
SiC-CDC NWs (molten salt)	1182	260	This work
Graphene sheets (molten salt)	~565	210-255	13
SiC-CDC (Cl_2-etching)	1531	54-141	14
Carbon NWs/fibers	152	170	15
SiC-CDC nanospheres (molten salt)	881	176	16

Additional references

1 X. Zou, X. Lu, Z. Zhou, W. Xiao, Q. Zhong, C. Li and W. Ding, *J. Mater. Chem. A*, 2014, **2**, 7421–7430.

2 X. Zou, X. Lu, Z. Zhou and C. Li, *Electrochem. Commun.*, 2012, **21**, 9–13.

3 X. Y. Yan and D. J. Fray, *Adv. Funct. Mater.*, 2005, **15**, 1757–1761.

4 X. Zou, K. Zheng, X. Lu, Q. Xu and Z. Zhou, *Faraday Discuss.*, 2016, **190**, 53–69.

5 L. Hu, Y. Song, J. Ge, J. Zhu and S. Jiao, *J. Mater. Chem. A*, 2015, **3**, 21211–21218.

6 A. M. Abdelkader, K. T. Kilby, A. Cox and D. J. Fray, *Chem. Rev.*, 2013, **113** , 2863–2886.

7 W. Xiao and D. Wang, *Chem. Soc. Rev.*, 2014, **43**, 3215–3228.

8 X. Zou, L. Ji, X. Yang, T. Lim, E. T. Yu and A. J. Bard, *J. Am. Chem. Soc.*, 2017, **139**, 16060–16063.

9 X. Jin, P. Gao, D. Wang, X. Hu and G. Z. Chen, *Angew. Chem. Int. Ed.*, 2004, **43**, 733–736.

10 X. Zou, L. Ji, X. Lu and Z. Zhou, *Sci. Rep.*, 2017, **7**, 9978.

11 H. V. Ijije, C. Sun and G. Z. Chen, *Carbon*, 2014, **73**, 163–174.

12 H. Yin, X. Mao, D. Tang, W. Xiao, L. Xing, H. Zhu, D. Wang and D. R. Sadoway, *Energy Environ. Sci.*, 2013, **6**, 1538–1545.

13 A. M. Abdelkader, *J. Mater. Chem. A*, 2015, **3**, 8519–8525.

14 P. Yan, J. Xu, C. Wu, Y. Gu, X. Zhang, R. Zhang and Y. Song, *Electrochim. Acta*, 2016, **189**, 16–21.

15 Y.-H. Hsu, C.-C. Lai, C.-L. Ho and C.-T. Lo, *Electrochim. Acta*, 2014, **127**, 369–376.

16 K. Zheng, X. Zou, X. Xie, C. Lu, S. Li and X. Lu, *Mater. Lett.*, 2018, **216**, 265–268.